

Targeting Peptidoglycan using Radiolabeled Click Chemistry for PET Infection
Imaging

by
Aryn Alanizi

THESIS

Submitted in partial satisfaction of the requirements for degree of
MASTER OF SCIENCE

in

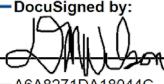
Biomedical Imaging

in the

GRADUATE DIVISION
of the

UNIVERSITY OF CALIFORNIA, SAN FRANCISCO

Approved:

DocuSigned by:

A6A8271DA18044C... David M Wilson
Chair

DocuSigned by:

Henry F. VAnBrocklin

DocuSigned by:
Robert Flavell
Robert Flavell

DocuSigned by:
Michael Evans
40E92A530F764EE... Michael Evans

Committee Members

Copyright 2020

by

Aryn Anne-Ayad Alanizi

Acknowledgements

I have received a great deal of support and assistance throughout the writing and execution of this thesis.

I would like to thank Dr. David Wilson for providing the opportunity to pursue this scientific endeavor. I am deeply grateful for your support, which has served as great motivation in the completion of this thesis.

I would also like to thank Dr. Matthew Parker, whose expertise was incredibly helpful in executing the research and whose knowledge was essential to developing the methodology. Your patience and invaluable experience were instrumental in filling my knowledge gaps.

I would like to extend many thanks to Dr. Alexandre Sorlin for assisting in the development of the materials necessary to accomplish this project. Your aid is greatly appreciated and your insight guided important conversations.

I would also like to express gratitude to my committee, Dr. Henry VanBrocklin, Dr. Michael Evans, and Dr. Robert Flavell for providing support and offering advice throughout this process.

Finally, I would like to extend a big “thank you” to my family, friends, and everyone else who has supported me. Your encouragement and support mean the world to me, especially throughout the COVID-19 pandemic.

Targeting Peptidoglycan using Radiolabeled Click Chemistry for PET Infection Imaging

Aryn Alanizi

Abstract

One of the major challenges in imaging bacterial infection using Positron Emission Tomography is the insufficiency of fluorine-18 labeled probes. Several carbon-11 D-amino acid probes have been developed to mimic bacteria-specific metabolic pathways and have been translated into the clinical realm.¹ However, the short half-life of carbon-11 limits its applicability and reach in examining populations of interest. Directly radiolabeled fluorine-18 probes have been synthesized but have been unsuccessfully translated to *in vitro* models, and thus a pressing need to fulfill this gap exists. Click chemistry, an indirect alternative tool to tag biomolecules, has been shown to tag and study molecules, including bacteria specific biomarkers such as peptidoglycan.² Utilizing the cell's biosynthetic machinery to incorporate essential components to peptidoglycan synthesis such as modified sugars or amino acids, these modified compounds can then selectively ligate to a second probe bearing a visible component.³ By utilizing these well-established bio-orthogonal techniques,⁴ we developed an optimized, high-throughput azide-alkyne click chemistry assay to indirectly label gram-positive *Staphylococcus aureus* and gram-negative *Escherichia coli* with three fluorine-18 PET tracers: [¹⁸F]FB-DBCO, [¹⁸F]PEG4-DBCO, and [¹⁸F]Sulfo-DBCO. Tracer ligation to D-azido-alanine, a modified D-alanine metabolite, via strain-promoted azide-alkyne cyclooctyne (SPAAC) addition was quantified to determine the efficiency of the fluorine-18 PET tracer and to propose the development of the next generation of PET tracers for infection imaging.

Table of Contents

Introduction	1
Materials and Methods.....	6
Results	12
Discussion.....	23
Conclusion	29
References	30

List of Figures

Figure 1. Chemical Structures of radiolabeled and azide derived D-amino acids.....	2
Figure 2. General schematic overview of Click PET bacteria cell wall labeling.	4
Figure 3. Chemical structure of a series of C-terminal modified D-azido-alanine derivatives for screening in Click PET assay.....	5
Figure 4. General reaction schematic of SFB-derived [¹⁸ F]-alkyne radiotracers.....	7
Figure 5. Initial Workflow Assay.....	9
Figure 6. Optimized High-Throughput Assay.....	11
Figure 7. <i>S. aureus</i> bio-orthogonal fluorophore labeling.....	12
Figure 8. First click chemistry uptake assay.....	13
Figure 9. Cellular ligations of 3 alkyne screen in <i>S. aureus</i> (SA) and <i>E. coli</i> (EC) subjected to different washing methods	15
Figure 10. Time course of SPAAC kinetics	17
Figure 11. Cellular signal with the maximum concentration of bacteria available for SPAAC ligation.....	18
Figure 12. Cellular fluorescence with the maximum concentration of bacteria available for SPAAC ligation.....	19
Figure 13. Fluorescence intensity of bacteria washed on cellulose acetate and nylon spin filters	20

Figure 14. Wash buffer removal of [¹⁸ F]Sulfo-DBCO alkyne binding.	21
Figure 15. Optimized high-throughput assay results	22

List of Tables

Table 1. 1:20 dilution of OD ₆₀₀ of maximal bacteria growth.....	18
---	----

Introduction

As microbial infections rise, a method to evaluate patient response to active infection is needed to monitor infection progression, especially in cases of antibiotic treatment given current trends of increasing resistance to broad spectrum antibiotics.⁵ In past years, imaging studies have sensed bacterial infections by relying upon abnormal physiologic changes in host tissues detected by imaging modalities such as Magnetic Resonance and Computed Tomography.² However, a reliable imaging modality to probe live bacterial infection is still an unmet clinical need as the current methods of detection rely on indirect consequences of infection like morphologic changes or host immune response.⁶

In recent years, several new imaging studies have put forth Positron Emission Tomography imaging probes specifically designed to target sites of active infection.⁷⁻¹⁰ These methods rely upon biochemical approaches to label active pathogenic infection sites while avoiding host tissues.

In creating PET probes, the need to label bacteria-specific pathways is essential to not only discriminate the etiology of inflammation from host-induced inflammation such as cancerous states, but to identify bacterial infection from fungal and viral. A biomarker of particular interest is peptidoglycan, an identifying cell-wall component of bacteria. Comprised of an abundance of sugars and peptide linkages, most bacteria produce and incorporate D-amino acids into the peptidoglycan and have served as the initiation of developing amino acid-derived PET tracers.¹¹ Our central hypothesis is that D-amino acids (DAA) could be used as specific markers for live bacterial infection *in vivo* using position emission tomography (PET). The Wilson Group at UCSF has developed D-[¹¹C]-

methionine (DMet) **1**, D-[^{11}C]-alanine (DAIa) **2**, and D-[^{11}C]-alanyl-D-alanine **3** as three bacteria-specific imaging probes (**Figure 1**).^{7,8}

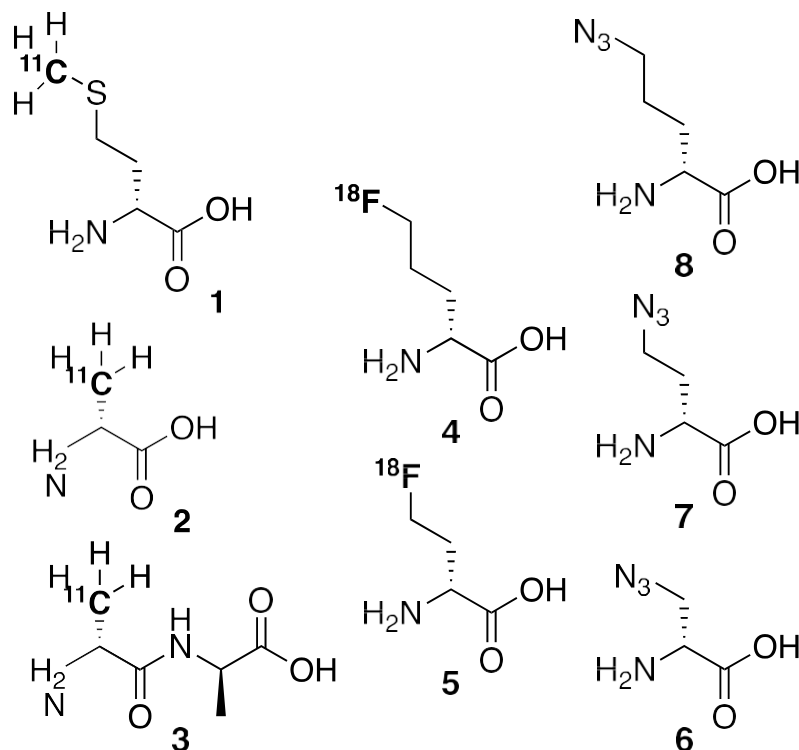


Figure 1. Chemical Structures of radiolabeled and azide derived D-amino acids. (1-3) [^{11}C]-Modified DAA can be used as a metabolite for visualizing bacterial cell wall using Positron Emission Tomography (PET). **(4-5)** [^{18}F]-modified DAA with no uptake when subjected to *in vitro* uptake assays. **(6-8)** Proposed D-azido-modified DAA for azide-alkyne click chemistry optical and PET imaging.

DMet is considered to be a first-generation tracer and has advanced to clinical trials. DAIa was put forth as a second-generation tracer and has since outperformed DMet in all preclinical experiments, but the enantiopure radiolabeled [^{11}C]DAIa is challenging to synthesize. Moreover, both tracers are carbon-11 derived and suffer from its short 20-

minute half-life, presenting challenges for accessing the diverse patient populations that could benefit from infection imaging.

The next generation tracer would greatly benefit from inclusion of fluorine-18, a positron emitting isotope with a 109.5-minute half-life. However, to date, all attempts to incorporate [^{18}F] into an amino acid-derived probe have failed. Particularly disappointing are DAla and DMet homologs **5** and **6** (**Figure 1**) that have been slightly modified at the side chain. Currently it is unknown why these compounds failed despite radiolabeling at intuitive positions, but more importantly, it is uncertain as to which molecules will succeed. Therefore, there is a need for a biochemical tool that will allow us to further understand how bacterial tracers are behaving and to provide insight into how to develop new PET imaging probes.

Metabolic click chemistry has been a widely established biochemical approach to tag and study molecules, including bacteria peptidoglycan.¹² Azide-derived D-amino acids, particularly D-azido-alanine and sugar metabolites have been demonstrated to incorporate into cell wall components to later be reacted with strain-promoted azide-alkyne cycloaddition (SPAAC) reactions such as cyclooctynes bearing chromophores and other chemical reporters.³ By applying metabolic click chemistry to overcome our current challenges in the direct radiolabeling of PET tracers, we hope to understand and develop new PET probes. Despite the wealth of data using optical chemical reporters, we used positron emission to detect D-azido amino acid probe incorporation to accelerate and inform imaging probe development for future translation to the clinical realm. Based upon a previously developed a high-throughput *in vitro* assay to screen PET tracers,¹³ we

implemented a similar workflow that would accumulate data faster than using optical approaches, but used optical methods to confirm click reaction progress (**Figure 2**).²

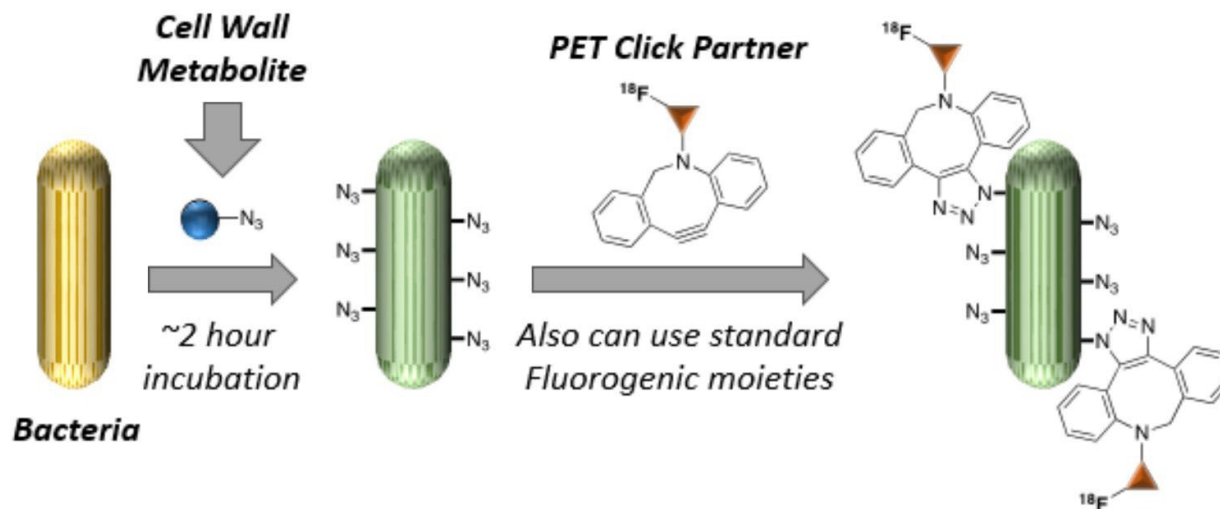


Figure 2. General schematic overview of Click PET bacteria cell wall labeling. Bacteria is incubated with azide-derived cell wall metabolite then tagged with a positron emitting cyclooctyne.

In this study, we focused on two pathogens: *Escherichia coli* (*E. coli*) and *Staphylococcus aureus* (*S. aureus*). *E. coli* is a gram-negative species and can be targeted by well-documented, established PET tracers such as [¹⁸F]-FDS,¹⁰ but can also be leveraged to discover specific, targeted PET imaging agents. *S. aureus* is a known causative pathogen of vertebral discitis osteomyelitis (VDO)¹⁴ and is a gram-positive model for monitoring radiolabeled amino acid uptake due to its large peptidoglycan-to-cell-mass concentration.⁷ By incorporating azide-containing D-amino acids in these bacterial species, we attempted to determine where the D-amino acids were used to identify a specific metabolic pathway for cellular uptake. Using these bacterial species as models for clinically relevant disease, their radioligand uptake may be localized and quantified in order to have a better understanding of the chemical incorporation of the

radiolabeled structural metabolites. Ultimately, these findings will aid in the creation of the next generation of PET tracers to target unique pathological strains. Using these bacterial systems and metabolic click chemistry, we had three objectives:

- 1) Use a series of azide-bearing linear D-amino acids (Compound **6**, **7**, and **8**) to correlate side chain length with bacteria incorporation.
- 2) Use Compound **6**, D-azido-alanine, to assess the cell wall fraction versus the cytosolic fraction of D-azido-amino acids within gram-positive and gram-negative pathogens.
- 3) Use click chemistry with a series of D-azido-amino acid derivatives of Compound **6** to screen for bacterial incorporation to identify potential new PET targets (**Figure 3**).

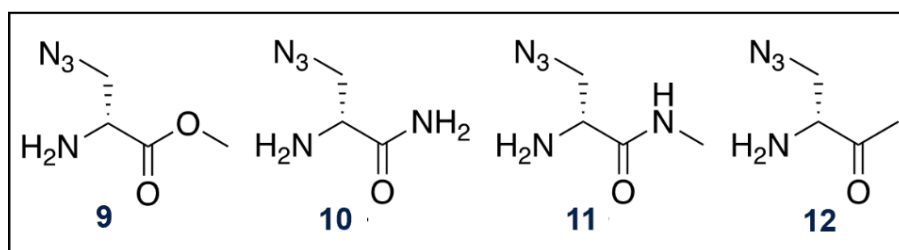


Figure 3. Chemical structure of a series of C-terminal modified D-azido-alanine derivatives for screening in Click PET assay. (9) Methyl ester D-azido-alanine. (10) Amide D-azido-alanine. (11) Methyl amide D-azido-alanine. (12) Methyl D-azido-alanine.

However, an optimized, efficient high-throughput click chemistry assay needed to be developed. Much focus will therefore be placed on completing Aim 1.

Materials and Methods

A. Strains and Reagents

The *S. aureus* strain ATCC 12600 and *E. coli* strain ATCC 25922 were used for all experiments. The metabolic labeling compound N β -Azido-D-2,3-diaminopropionic hydrochloride acid (D-azido-alanine, compound **6**) was acquired from Chem-Impex (Wood Dale, Illinois). DBCO-MB-543 cyclooctyne fluorophore, Cy 5.5 cyclooctyne fluorophore, AlexaFluor Dye 488 DBCO (AF488), and azide and alkyne agaroses were obtained from Click Chemistry Tools (Scottsdale, AZ). Buffer Solution pH 8.00 was obtained from Thermo Fisher Scientific (Waltham, MA). F-12, Phosphate Buffered Saline (PBS), Fetal Bovine Serum (FBS), and Mg-free Dulbecco's Phosphate Buffered Saline (DPBS) were acquired from Gibco (Dublin, Ireland). M9 minimal medium, Tween-20, and D-alanine were obtained from Sigma-Aldrich (St. Louis, MO). Luria Broth (LB) and agar plates were obtained from Tecknova (Hollister, CA).

B. Instrumentation

All optical click experiments were analyzed on the Genentech FlexStation® 3 Multi-Mode Microplate Reader from Molecular Devices (San Jose, CA) at the UCSF Mission Bay campus. All radiotracer click experiment emission data was analyzed on the Hidex Automatic Gamma Counter from Hidex (Turku, Finland) at the UCSF China Basin campus. Optical densities were taken on GENESYS™ 20 Visible Spectrophotometer from Thermo Fisher Scientific (Waltham, MA).

C. Radiolabeled Alkyne Syntheses

The cold click chemistry alkyne standards were derived from commercially available N-succinimidyl 4-fluorobenzoate (SFB). 1 equivalent of cold SFB was reacted with diethylformamide (DMF) and triethylamine (TEA) and purified by preparatory HPLC.

[¹⁸F]SFB was prepared from an automated radiosynthesis process.¹⁵ Due to its rather simplistic production, it served as a convenient prosthetic group to generate 3 alkynes under mild reaction conditions. Amine precursors were stoichiometrically added to triethylamine and DMF to generate three [¹⁸F]-labeled alkynes: [¹⁸F]FB-DBCO, [¹⁸F]PEG4-DBCO, and [¹⁸F]Sulfo-DBCO. [¹⁸F]FB-DBCO (**Figure 4A**) was synthesized from the acylation of a commercially available primary amine following established protocols.¹⁶ [¹⁸F]PEG4-DBCO was synthesized via tosylation of commercially available PEG4-DBCO.¹⁷ [¹⁸F]Sulfo-DBCO was a newly synthesized alkyne using sulfo-DBCO precursor material.

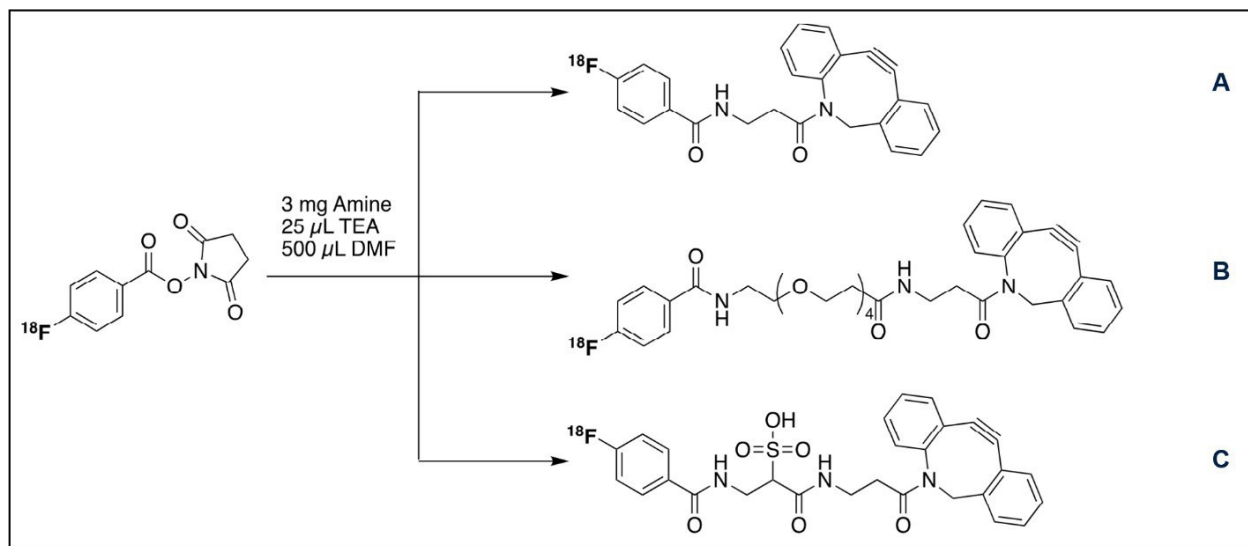


Figure 4. General reaction schematic of SFB-derived [¹⁸F]-alkyne radiotracers. (A) [¹⁸F]FB-DBCO chemical structure. **(B)** [¹⁸F]PEG4-DBCO chemical structure. **(C)** [¹⁸F]Sulfo-DBCO chemical structure.

D. General Metabolic label incorporation into bacteria

Frozen glycerol stocks of bacteria were streaked onto agar plates and incubated at 37°C overnight or until individual colonies were visible. A single, isolated colony of bacteria was collected and added to 50 mL of LB in a 250 mL culture flask and incubated at 37°C and shaken at 180 rpm overnight. An aliquot of the overgrown culture was diluted to a final volume of fresh LB in a 50 mL culture tube and shaken at 180 rpm at 37°C for 3-4 hours (**Figure 5**). Unless otherwise stated, an aliquot of the subculture was reconstituted in 8 mL of F-12 medium containing a 5 mM final concentration of compound **6** or D-alanine metabolite¹⁷ in Buffer Solution (pH 8.00) and shaken at 180 rpm at 37°C for 1 hour. The bacteria solution was decanted into a 15 mL centrifuge tube and pelleted at centrifugation settings of 8000 rpm for 5 minutes, unless otherwise stated. The pellet was reconstituted and washed with buffer (WB: 2% v/v FBS, 0.05% v/v Tween-20, DPBS)¹⁷ three times, unless otherwise stated. The pellet was reconstituted in PBS to prepare for alkyne ligation reaction.

E. Bacteria click reaction with [¹⁸F]cyclooctyne derivatives

Unless otherwise noted in optimized click assay method, azide-labeled bacteria in 1 mL of PBS was aliquoted into 1.5 mL microcentrifuge tubes where 50 µL of [¹⁸F]cyclooctyne derivative in PBS (185kBq) was added and shaken at 180 rpm at 37°C for 1 hour. 400 µL of mixture was transferred to a cellulose acetate Costar Spin-X filter tube from Corning (Corning, NY) and centrifuged at 8,000 rpm for 5 minutes. The filter was washed with WB (300 µL) then transferred to a separate collection tube where it was washed twice more. The filter portion and filtrate portions were separated and analyzed

on the Hidex. SPAAC Ligation was reported as a percentage of cellular signal to the sum total of cell and filtrate signal.

F. Bacteria click reaction with cyclooctyne fluorophore derivatives

Unless otherwise noted in optimized click assay method, azide-labeled bacteria in PBS were aliquoted into 1.5 mL microcentrifuge tubes (500 μ L) and 500 μ L of a 1% cyclooctyne fluorophore derivate in PBS was added and the mixture was shaken (180 rpm) at 37°C for 1 hour. The mixture was pelleted at 8,000 rpm for 5 minutes. The pellet was reconstituted and washed with WB three times then reconstituted in PBS, aliquoted onto a 96-well plate, and analyzed on a fluorescent plate reader (Flexstation III).

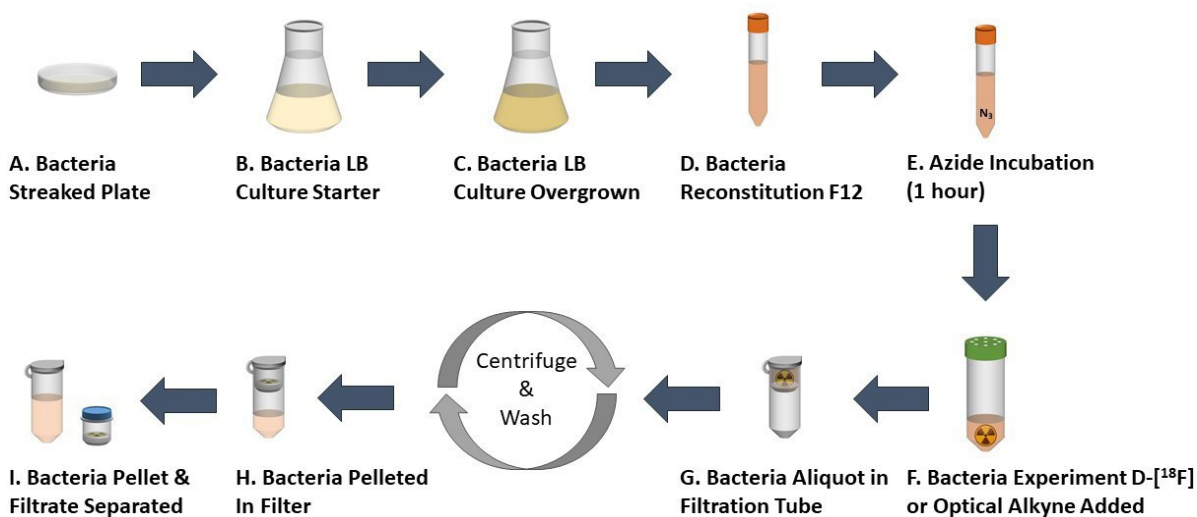


Figure 5. Initial Workflow Assay. Initial experiments were performed with this non-optimized workflow to attach alkyne to azide-incubated bacteria.

G. Optimized metabolic label incorporation into bacteria

Frozen glycerol stocks of bacteria were streaked onto agar plates and incubated at 37°C overnight or until individual colonies were visible. A single, isolated colony of bacteria was collected and added to 50 mL of LB in a 250 mL culture flask and incubated

at 37°C and shaken at 180 rpm overnight. A 150 µL aliquot of the overgrown culture was diluted 1:100 (15 mL) of fresh LB in a 50 mL culture tube and shaken at 180 rpm at 37°C for 3 hours to mid-logarithmic phase (OD 0.4-0.9 at 600 nm) (**Figure 6**). 9 mL of mid-log bacteria were aliquoted to new cell culture tubes and 1 mL of a 5 mM (final concentration) of the indicated azide or buffered DAla vehicle was added to each culture tube. The solution was shaken at 180 rpm at 37°C for 1 hour. The bacteria cells were decanted into a 15 mL centrifuge tube and pelleted by centrifugation at 8,000 x g for 5 minutes or until a sizeable pellet formed. The pellet was resuspended in 500 µL of WB buffer and transferred to a 1.5 mL microcentrifuge tube where it was subsequently washed 4 more times at 12,000 x g for 2 minutes. The washed pellet was reconstituted in 1 mL of PBS to prepare for the alkyne ligation reaction.

H. Optimized bacteria click reaction with [¹⁸F]cyclooctyne derivatives

From the 1 mL PBS solution of azide-labeled bacteria, 500 µL was removed and re-aliquoted into a separate 1.5 mL microcentrifuge tubes. Click controls were prepared in additional 1.5 mL microcentrifuge tubes from 100 µL of thoroughly aspirated azide agarose beads (positive control) and alkyne agarose beads (negative controls) displaced in 900 mL of PBS. 500 µL of [¹⁸F]cyclooctyne derivative was delivered in PBS vehicle (185kBq) and shaken at 180 rpm at 37°C for 1 hour. 200 µL of mixture was transferred to a cellulose acetate Costar Spin-X filter tube from Corning (Corning, NY) and centrifuged at 12,000 x g for 2 minutes. The spin filter tubes were washed with WB (300 µL) at the same centrifuge settings. The filter and filtrate portions were separated and analyzed on the Hidex. SPAAC Ligation was reported as a percentage of cellular signal to the sum

total of cell and filtrate signal. Optical densities were assessed at 600 nm in a 1:20 PBS dilution.

I. Optimized bacteria click reaction with cyclooctyne fluorophore derivatives

From the 1 mL PBS solution of azide-labeled bacteria, the remaining 500 μ L was treated with 500 μ L of a 1% cyclooctyne fluorophore derivative in PBS vehicle and shaken at 180 rpm at 37°C for 1 hour. The mixture was pelleted at 12,000 x g for 2 minutes. 100 μ L of the parent liquid was transferred to a 96-well plate or saved in a microcentrifuge tube. The remaining liquid was decanted and the pellet was reconstituted and washed in WB 2 times at 12,000 x g for 2 minutes. The washed pellet was reconstituted in 1 mL PBS, aliquoted onto a 96-well plate, and analyzed on a fluorescent plate reader (Flexstation III).

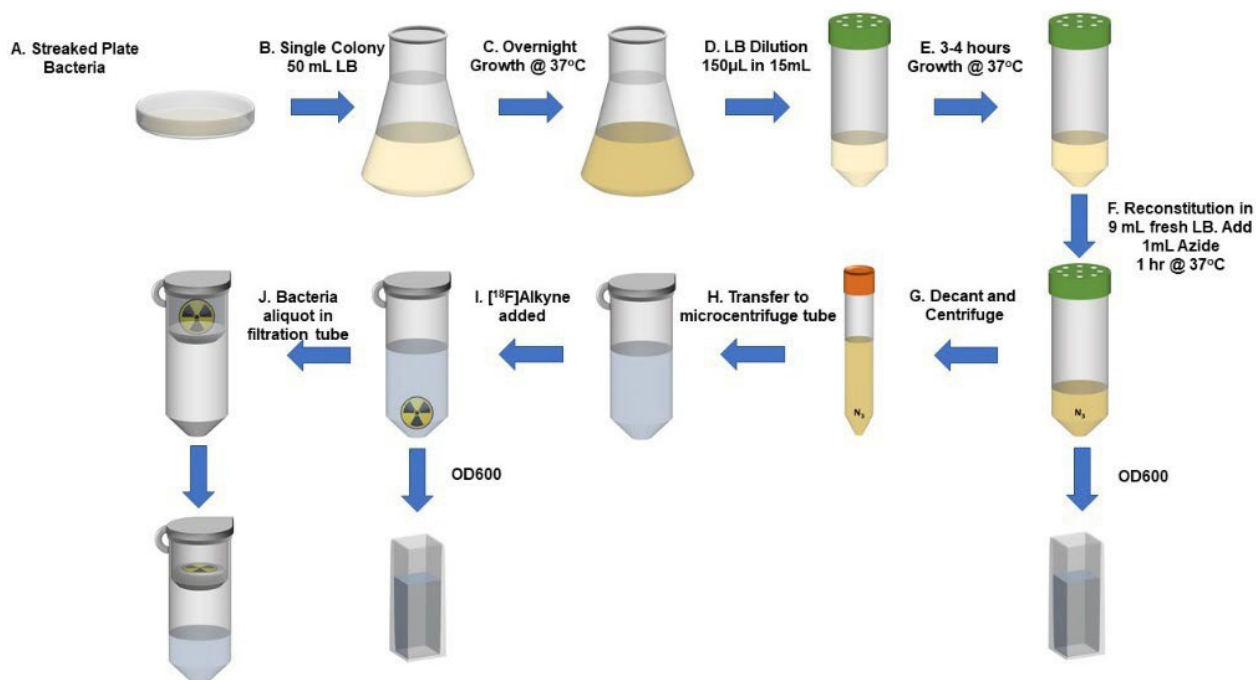


Figure 6. Optimized High-Throughput Assay. Workflow for high-throughput *in vitro* assay for labeling bacterial cell wall with azide-derived metabolites followed by ligation with positron emitting or fluorophore cyclooctyne. OD₆₀₀s may be taken along the way to

monitor growth state. Of particular note is step D, a necessary 1:100 dilution to grow bacteria to a metabolically active state.

Results

To develop a method for bio-orthogonally radiolabeling *S. aureus* and *E. coli* using strain-promoted azide-alkyne cycloaddition (SPAAC), we screened a series of standard fluorogenic alkynes specific to ligate with their azide click partner, D-azido-alanine.¹⁷ Bacteria were prepared following our workflow assay (**Figure 5**) where cells were incubated for 3 hours in 4 media types: PBS, M9, F-12, and LB. Log-phase bacteria were incubated with D-azido-alanine or DAla. After washing out unincorporated metabolites, *S. aureus* cells were treated with alkynes MB 543 ($\lambda_{\text{ex/em}}$ 544/560 nm) and Cy 5.5 ($\lambda_{\text{ex/em}}$ 678/694 nm) that fluoresce in the visible light spectrum (**Figure 7B, 7C**). Compared to cells grown with DAla metabolic label, we found that D-azido-alanine incorporated by *S. aureus* and *E. coli* only underwent SPAAC reactions with alkynated fluorophores. The absence of fluorescence in cells incubated with DAla indicated specificity for azide compounds and established DAla as a negative control independent of growth media.

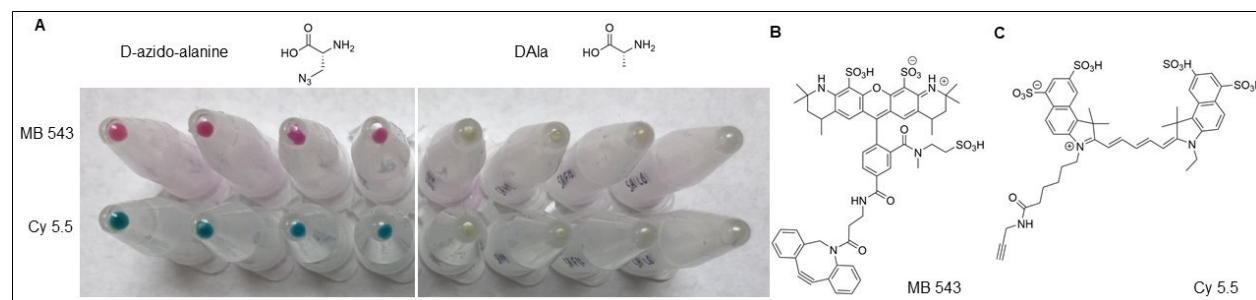


Figure 7. *S. aureus* bio-orthogonal fluorophore labeling. (A) A series of SPAAC reactions in *S. aureus* grown (left to right) in PBS, M9, F-12, and LB. D-azido-alanine can be visibly seen when it ligates with alkyne-labeled fluorophore partners. DAla, a negative control metabolite, does not react with fluorophores bearing alkynes. (B) Chemical structure of MB 543 cyclooctane alkyne (pink). (C) Chemical structure of Cy 5.5 fluorophore alkyne (blue).

Next, we sought to explore radiolabeled alkyne click partners and used optical results to confirm our PET findings. N-succinimidyl 4- ^{18}F fluorobenzoate (SFB), a common commercially available radiolabeling prosthetic was used to synthesize a preliminary ^{18}F FB-DBCO alkyne (**Figure 4A**) to test feasibility of concept. Using the preestablished workflow assay (**Figure 5**), we performed radioactive uptake assays where we first incubated *S. aureus* with varying concentrations of D-azido-alanine and clicked bacteria to ^{18}F FB-DBCO. Initial uptake assays yielded a disappointing 2-4% azide- alkyne ligated reaction in the cellular pellets (**Figure 8**). Though there was a slight trend of increased SPAAC ligation on bacterial pellets, this was not found to be statistically significant. However, reported concentrations of 5 mM have proven to be successful in optical click chemistry *in vitro* assays so we maintained future use of 5 mM azide concentrations.¹⁷ Azide agarose was used as a positive control to set the upper limit of measurable activity. Nonspecific binding was highly prevalent as the percentage of SPAAC reaction was much lower than the minimum PET signal set by the negative agarose control.

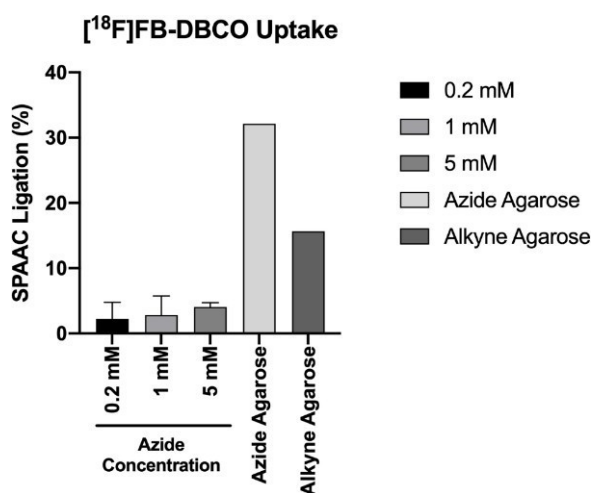


Figure 8. First click chemistry uptake assay. Varying molar concentrations of D-azido-alanine were incubated with *S. aureus*. Despite increased ligation at higher molar

concentrations, this trend was not statistically significant. Azide agarose beads and alkyne agarose beads were used as a set of positive and negative standard controls, respectively.

Since previous optical click chemistry experiments confirmed SPAAC reactions with multiple fluorophore-bearing alkynes on both bacterial strains, we sought to determine if multiple PET alkyne tracers could ligate to the azide in an attempt to increase PET tracer signal. A panel of SFB-derived [^{18}F] radiolabeled alkynes (**Figure 4**) with structural amine changes were created to improve water solubility and increase the partitioning coefficient in order to understand if the simplest PET alkyne click partner, [^{18}F]FB-DBCO, was amenable to chemical changes.

To test this, water-insoluble [^{18}F]FB-DBCO PET tracer was screened against [^{18}F]PEG4-DBCO (**Figure 4B**) and [^{18}F]Sulfo-DBCO (**Figure 4C**) in *S. aureus* and *E. coli*. Bacteria were grown to mid-log phase with D-azido-alanine or DAAla. Metabolite cultures and agarose control beads were incubated with each PET alkyne tracer.

Ligated bacterial reactions were then washed using three different conditions to compare washing method efficiency. Bacteria were washed on nylon or cellulose acetate Spin-X filters or manually pelleted and washed to mimic optical processing in an attempt to minimize previously observed nonspecific binding (**Figure 8**).

To determine background activity levels, 100 μL of each PET tracer was added to blank PBS spin-filters and subtracted from overall activity in each experiment. An initial glance at the data suggests that spin filtering methods are better at collecting ligated SPAAC reactions than manually pelleting and washing bacteria (**Figure 9**). Upon analysis, the cellulose acetate spin filtering method was shown to capture more ligated reactions

compared to its nylon spin filter counterpart and was selected for future separations of bacteria and filtrate.

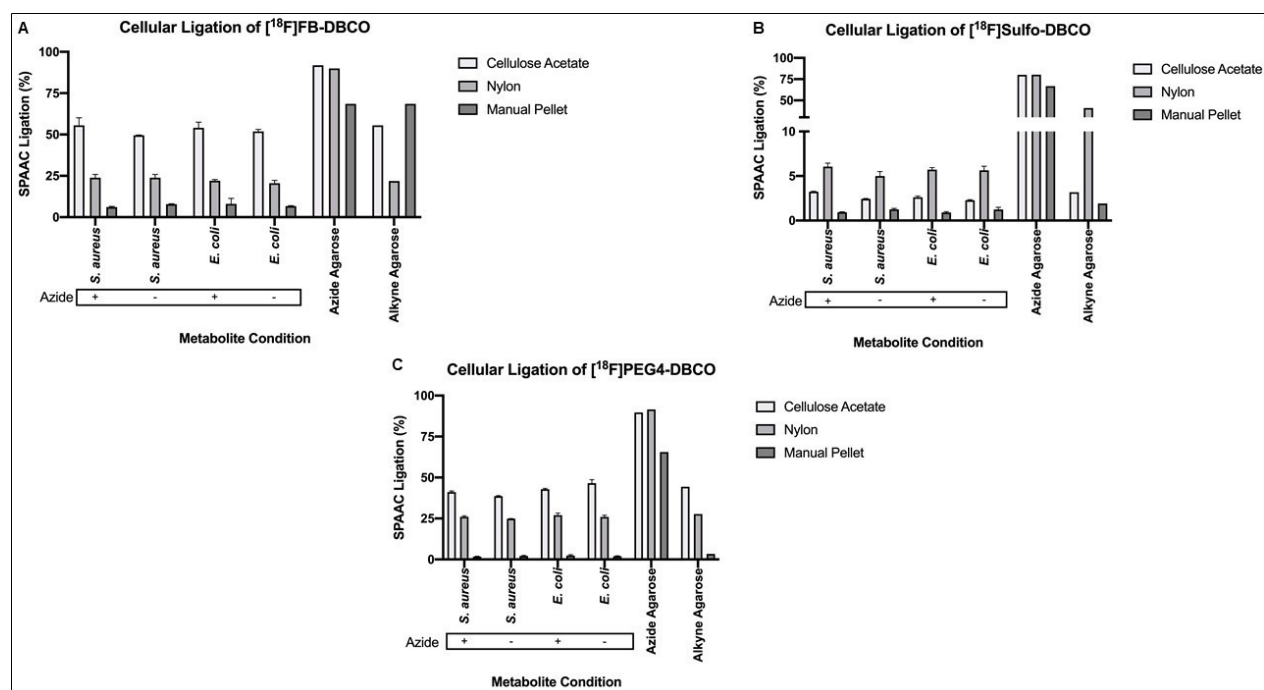


Figure 9. Cellular ligations of 3 alkyne screen in *S. aureus* (SA) and *E. coli* (EC) subjected to different washing methods. Each pathogen was incubated with D-azido-alanine and DAla. Azide agarose and alkyne agarose beads reflect maximum and minimum ligation percentage possible per alkyne. **(A)** The ligation of [¹⁸F]FB-DBCO, our original PET tracer, shows high uptake in cellular pellets of both *S. aureus* and *E. coli*, however nonspecific binding is highly evident with minimal discernible differences between pathogens on any bacterial filtration method. **(B)** Ligation of [¹⁸F]Sulfo-DBCO similarly displays nonspecific binding, however the positive and negative agarose controls display a large dynamic range of variability. **(C)** [¹⁸F]PEG4-DBCO ligates to a lesser degree than [¹⁸F]FB-DBCO. Nonspecific binding across both pathogens and a small dynamic range across all filtration systems suggest poor application for future *in vitro* systems.

The radiolabeled alkyne screen demonstrated mixed results. [¹⁸F]FB-DBCO had the highest PET signal compared to [¹⁸F]PEG4-DBCO and [¹⁸F]Sulfo-DBCO; however, our positive and negative controls showed a rather tight dynamic window in observable signal.

Despite ligating 20-fold less than [^{18}F]FB-DBCO tracer and 16-fold less than water soluble [^{18}F]-PEG4-DBCO, [^{18}F]Sulfo-DBCO showed the least occurrences of nonspecific binding. Amongst the panel of alkynes tested, agarose controls incubated with [^{18}F]Sulfo-DBCO maintained the largest dynamic range of activity uptake of 76.91% from upper to lower limits on cellulose acetate spin filters. However, on average, only 2.6% of the radiolabeled alkyne ligated to D-azido-alanine in *E. coli* and *S. aureus* cultures. Similar uptake patterns presented in the negative control conditions and it remained unclear if [^{18}F]Sulfo-DBCO induced SPAAC or if it remained nonspecifically bound to bacterial pellets. However, due to the impressive dynamic range seen on agarose controls incubated with [^{18}F]Sulfo-DBCO compared to other screened [^{18}F]-labeled alkynes, [^{18}F]Sulfo-DBCO was selected for future optimized SPAAC reactions.

Because SPAAC speed is critical to find optimal alkyne incubation time, we established a bio-orthogonal kinetic assay for determining ligation incubation conditions. This time course uptake assay was performed under varying bacterial concentrations to determine if *S. aureus* growth phases and conditions permit azide incorporation and the alkyne reaction time. Our high-throughput uptake assay was utilized to incorporate metabolites into bacteria and ligate [^{18}F]Sulfo-DBCO. After azide incubation, four bacteria culture concentrations were created by 1:2 serial dilutions starting from a highly concentrated subculture to mid-log bacteria at an OD_{600} of 0.45 (0.45, 0.225, 0.1125, 0.05625). A negative control was prepared at OD_{600} 0.45, the same concentration as the maximum azide metabolite condition. At 10, 20, and 40 minutes, a set of SPAAC reactions was pulled for radioactivity ligation analysis. An aliquot of each concentration was collected by centrifugation and the pellet was washed and separated from the filtrate for

analysis. At 80 minutes, the last set of SPAAC reactions, negative control, and agarose controls were pulled (**Figure 10**).

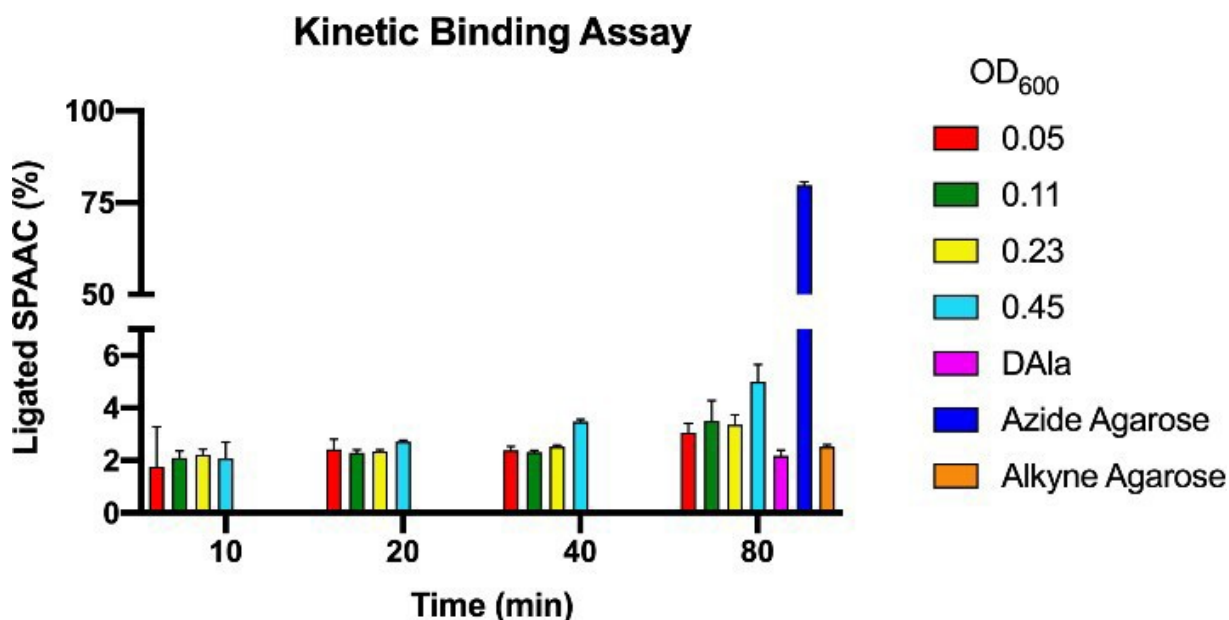


Figure 10. Time course of SPAAC kinetics. Varying amounts of *S. aureus* were created by a 1:2 dilution series measured by OD₆₀₀. These subcultures were ligated with [¹⁸F]Sulfo-DBCO. SPAAC ligation was monitored at 10-, 20-, 40-, and 80-minute pulls. Controls were only pulled at 80 minutes.

Over the time course, we observed a general increase in SPAAC reactions at later timepoints. Interestingly, we found that higher concentrations of bacteria correlated to greater [¹⁸F]Sulfo-DBCO uptake in the cell pellet with a 5% increased cellular ligation compared to previous uptake assay experiments. Encouraged by this data, we sought to increase the concentration of starting bacteria to increase azide incorporation and the number of available sites for the PET alkyne partner to bind.

We subsequently quantified the maximum amount of bacteria that could grow within the permissible time constraints of operating with a decaying [¹⁸F] PET tracer. Bacterial cultures from the high-throughput assays were altered from a 2:9 overnight culture to LB to a 1:9 dilution to encourage sustained exponential growth in conditions

with plentiful medium. After metabolic labeling, entire cultures were pelleted, thoroughly washed, and resuspended in 1 mL of PBS for alkyne ligation. After incubation, growth was assessed by OD600s (Table 1).

Table 1. 1:20 dilution of OD₆₀₀ of maximal bacteria growth.

	D-azido-alanine	DAla
<i>S. aureus</i>	0.703	0.849
	0.731	0.944
	0.783	0.848
<i>E. coli</i>	0.616	0.683
	0.634	0.677
	0.527	0.665

Increasing the amount of bacteria observed in our kinetic binding assay (**Figure 10**) also increased the observable PET signal from SPAAC ligation. However, indiscriminate [¹⁸F] signal presented in both metabolic conditions (**Figure 11**). Disappointingly, there was also undifferentiable signal between pathogens with near 1:1 SPAAC reactions on *E. coli* and *S. aureus*, conflicting with previous bio-orthogonal techniques translating to greater signal in higher peptidoglycan-containing pathogens.¹⁸

Max Bacterial [¹⁸F]Sulfo-DBCO Ligation

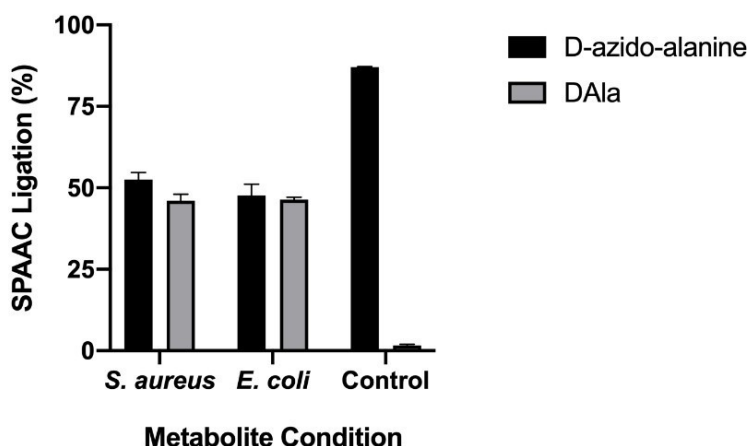


Figure 11. Cellular signal with the maximum concentration of bacteria available for SPAAC ligation. The maximum amount of *S. aureus* (SA) and *E. coli* (EC) that could grow within our time constraints were incubated with D-azido-alanine and DAla

metabolites and ligated with [^{18}F]Sulfo-DBCO alkyne. Though the azide and alkyne agarose controls (D-azido-alanine and DAAla mock conditions, respectively) established a wide range of ligation variability, incubating dense bacterial cultures with the radiotracer led to indiscernible differences in gram-positive and gram-negative bacteria and in metabolite conditions.

Because we had been able to determine SPAAC with great accuracy when alkynes were attached to fluorophore moieties, we reverted to optical click chemistry techniques to understand the observed nonspecific binding. Similar to the PET experiment, we investigated the upper limit of bacteria available for metabolic labeling and found OD_{600} growth trends to be consistent with previous PET assays. Surprisingly, AlexaFluor488 DBCO labeling demonstrated similar nonspecific binding trends despite our historic success in using optical techniques as a reliable observable signal (**Figure 12**).

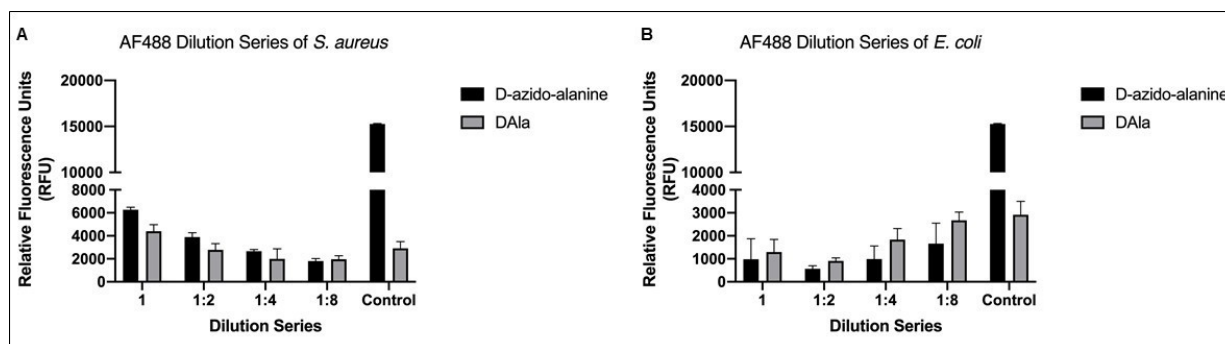


Figure 12. Cellular fluorescence with the maximum concentration of bacteria available for SPAAC ligation. The maximum number of bacteria that could grow within our time constraints was serially diluted from OD values (Table 1), incubated with D-azido-alanine and DAAla metabolites, and ligated with AF488 alkyne. Azide agarose (mimic of azide conditions) and alkyne agarose (mimic of DAAla conditions) served as a standard set of controls. **(A)** *S. aureus* ligation to AF488 measured by fluorescence intensity of cellular pellets. **(B)** *E. coli* ligation demonstrates variability across each bacterial concentration with no evident trend.

We attempted to repeat this optical experiment to determine if previously eliminated nylon spin filter tubes were more conducive to washing greater amounts of bacteria (**Figure 9**). AF488 was incubated with bacteria and the parent liquid was

analyzed on the plate reader from both spin filter tube conditions. However, we still could not eliminate the nonspecific binding of alkyne label as *S. aureus* and *E. coli* showed insignificant differences in SPAAC reactions with AF488 alkyne (**Figure 13**).

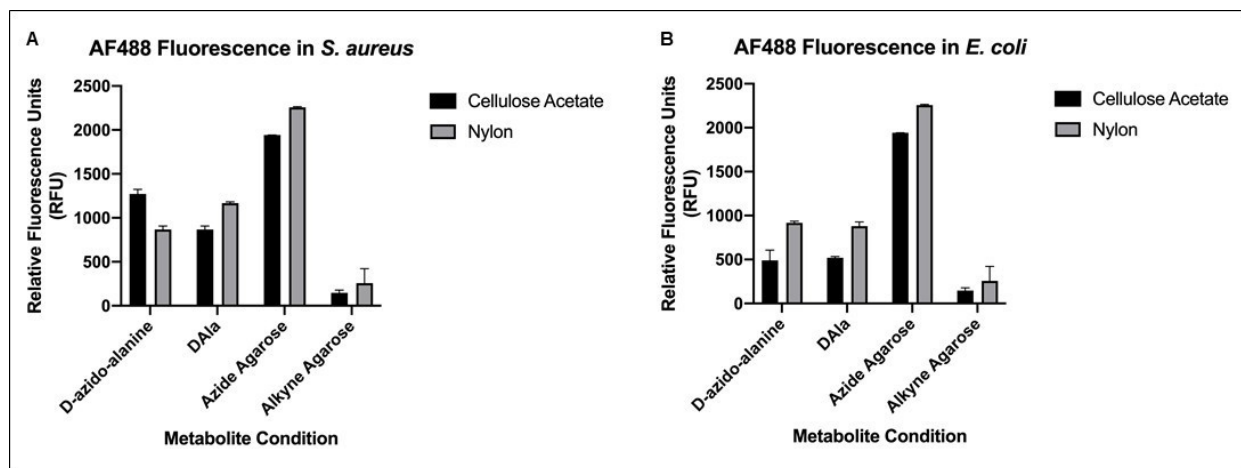


Figure 13. Fluorescence intensity of bacteria washed on cellulose acetate and nylon spin filters. *S. aureus* and *E. coli* were incubated with D-azido-alanine and DAla metabolites and ligated with AF488 alkyne. **(A)** *S. aureus* demonstrates good variability of SPAAC on cellulose acetate spin filters; however, an opposite trend of click reaction is apparent on nylon filters. **(B)** *E. coli* presents no SPAAC ligation differences between metabolite conditions on both spin filtering methods.

Several washing methods were revisited to investigate the efficiency of our WB in removing excess alkyne. An in-depth literature search uncovered four commonly utilized washing solutions: PBS, M9, LB, and F-12.^{19,20} PET click assays were repeated by cross-examining these wash solutions to our WB (**Figure 14**). Despite high bio-orthogonal ligation upwards of 60%, we continued to observe nonspecific binding of [¹⁸F]Sulfo-DBCO with each wash solution in both pathogens and in both cell metabolic labeling conditions. It was determined that we could not remove non-ligated [¹⁸F]Sulfo-DBCO at this concentration of bacteria.

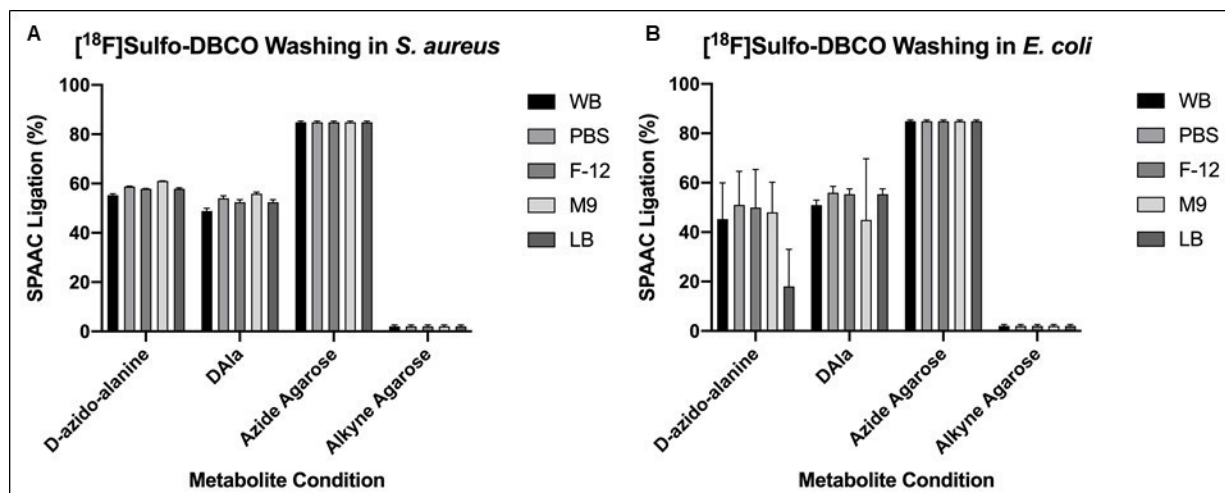


Figure 14. Wash buffer removal of $[^{18}\text{F}]$ Sulfo-DBCO alkyne binding. 5 different wash solutions were used to thoroughly remove excess alkyne. Each wash solution was tested on D-azido-alanine cultures and DAla cultures. Azide and alkyne agarose controls demonstrated stark differences in SPAAC ligation with each wash solution. **(A)** *S. aureus* shows similar ligation percentages across all four washing media with little variability; however, there are almost no differences between SPAAC ligation on D-azido-alanine- and DAla- containing bacterial cultures. **(B)** Minimal differences in *E. coli* are present amongst wash solutions.

In recent efforts, we canvassed optimal bacterial concentrations in an attempt to minimize nonspecific binding while maximizing signal output. Revisiting the literature led to the discovery of a reported 1:100 *S. aureus* subculture for optical click experiments.¹⁷ We repeated our high-throughput uptake assay with *S. aureus* at this concentration in LB and F12 subculture media to grow bacteria to mid-log phase (OD_{600} 0.4-0.7) over a 1-hour period. A final concentration of 5 mM buffered metabolite solution was incubated in each subculture. Excess metabolite was washed off and *S. aureus* was committed to incubation in a $[^{18}\text{F}]$ Sulfo-DBCO arm or AF488 optical arm (**Figure 15**).

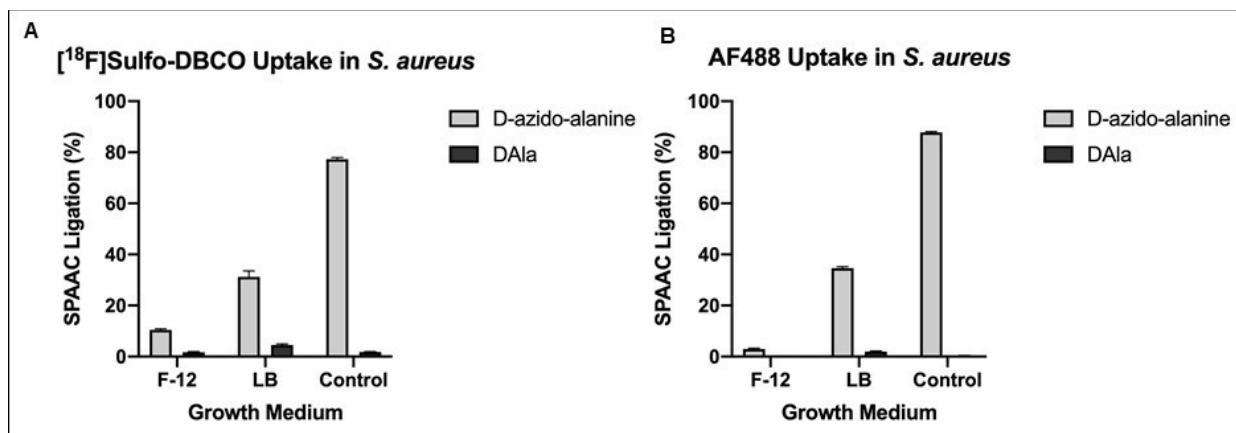


Figure 15. Optimized high-throughput assay results. D-azido-alanine and DAla metabolites were incubated with radioactive alkyne, [^{18}F]Sulfo-DBCO, and fluorophore alkyne, AF488. Azide and alkyne agarose beads were used for mimicking D-azido-alanine and DAla conditions. **(A)** [^{18}F]Sulfo-DBCO ligation in optimized assay. Subcultures grown in F-12 and LB shows higher ligation in both media and noticeable differences in metabolite conditions. **(B)** AF488 ligation in optimized assay. Saved cellular pellets were resuspended in 1 mL of PBS. The cellular pellet fraction was taken as a percentage of the sum of the pellet and unligated AF488 alkyne parent filtrate. Fluorescence intensity differences are perceivable in metabolite and media type.

S. aureus subcultured in LB expressed 20% higher PET signal compared to subcultures grown in F-12 cell medium. This difference was also seen in the parallel optical arm where a similarly high 11.5-fold difference in fluorescence intensity was observed in SPAAC ligated AF488 in bacteria grown in LB compared to F-12 medium. Most importantly, this concentration of bacteria seemed to eliminate the nonspecific binding we could not previously execute while maintaining the broad dynamic range of observable PET activity signal and fluorescence intensity on agarose controls. These results are especially convincing as AF488 dye was visible on azide-labeled bacteria and not in the negative agarose control.

Discussion

An [^{18}F]-D-amino acid bacteria-specific PET imaging probe is needed, but attempts to directly radiolabel D-amino acids have proven to be challenging and are unable to label bacteria. In this study, we developed a high-throughput bio-orthogonal click chemistry assay and evaluated its performance *in vitro* in gram-positive and gram-negative bacteria models. This optimized high-throughput assay has several variables that, when manipulated, dramatically alter the characteristics of the SPAAC reaction and the interpretation of observable signal. Filtration separation technique, alkyne solubility, bacteria concentration, and alkyne probe (PET and Optical) were variables found to be critical to the results obtained in the assay.

A. Filtrate Separation

We observed much greater signal in PET and optical click experiments using spin filtering methods, especially such in cellulose acetate Spin-X filters. Because cellulose acetate filters are composed of a thin membrane of cellulose triacetate and diacetate, they have low static charge and poor aqueous extractability while nylon filters are hydrophilic. These differences may attribute to the variability in the signal output in PET experiments. Due to the hydrophilic nature of nylon filters and highly aqueous cellular components, WB, and buffered vehicle, nylon filters may be conducive to bacterial passage through the filter. Nylon filters also have strong protein binding properties²¹ which may capture DAla or D-azido-alanine linkages. However, the filter pore diameter is larger than cellulose acetate filters, and may permit bacteria to pass through while capturing noncellular SPAAC reactions of modified amino acids, resulting in a narrowed signal

dynamic range. Cellulose acetate spin filters are hydrophobic and prevent aqueous filtrate from passing through the membrane and do not bind to proteins. The potential for a high dynamic range was seen with the use of cellulose acetate spin-filter tubes, suggesting better compatibility with this experiment. Because cellulose acetate filters provided the potential for higher separation in signal between D-azido-alanine and DA₁a cultures, these spin filters were selected to separate bacterial pellets from the filtrate.

Furthermore, the “high-throughput” component to this click assay places a strong emphasis on a rapid means of screening SPAAC reaction efficiency on bacteria. The spin filter method allows for rapid, successive washing and does not require transferring of any liquid, removing pipetting errors and loss of liquid or pellet. This is even more important given our liquid and pellets are radioactive. Therefore, spin filters are far more advantageous in separating bacteria from parent filtrate compared to manual pelleting and washing methods due to the rapid yet simplistic nature of the assay.

B. [¹⁸F] Alkyne Screen

Compared to [¹⁸F]FB-DBCO and [¹⁸F]PEG4-DBCO, [¹⁸F]Sulfo-DBCO ligated the poorest amongst the three. However, in the final optimized experiment (**Figure 15**), we observed D-azido-alanine and [¹⁸F]Sulfo-DBCO click partners specifically radiolabel *S. aureus* with low levels of nonspecific binding to non-azide containing bacteria and higher percent ligation than early cross-examinations to [¹⁸F]FB-DBCO and [¹⁸F]PEG4-DBCO. This may be partly explained by the resolution of nonspecific binding in our optimized experimental assay. However, [¹⁸F]Sulfo-DBCO also demonstrated a good dynamic window to differentiate agarose controls where the other PET tracers failed to do so,

suggesting a difference in its chemical composition that made it more compliant to the uptake assay protocol.

From the chemical structure of [¹⁸F]FB-DBCO, it is highly evident that it lacks hydrophilic prosthetic groups. Because the alkyne is delivered in PBS vehicle, a water-based salt solution, there is minimal evidence to suggest solubility. Furthermore, bacteria are prepared for alkyne ligation in the same aqueous environment. It can therefore be suggested that the incompatibility of solubility profiles may contribute to the highly prevalent nonspecific binding instances seen in early experiments.

[¹⁸F]PEG4-DBCO has been shown to have good solubility in similar bacterial models in optical click experiments where the length of the PEG-DBCO repeat units was assessed to be optimal for solubility at $n = 3$ ($C_{2n}H_{4n+2}O_{n+1}$), or 4 PEG units.¹⁷ However, the high prevalence of irreversible nonspecific binding in different wash steps, including WB and PBS, indicates its poor solubility in our bacteria models, which may be slightly altered by the presence of [¹⁸F].

[¹⁸F]Sulfo-DBCO seems to offer the best solubility profile of the three alkynes. The sulfate group attached to an alpha carbon increases the alkyne's solubility in aqueous environments, such as the cytosolic component of bacteria or alkyne vehicle delivery (PBS). Interestingly, the fluorophore alkynes MB 543 and Cy 5.5 (**Figure 7**) have numerous sulfate groups and were shown to specifically bind to the azide *in vitro*. However, bulky, sterically hindered regions also contribute hydrophobicity to two regions of the molecule which would decrease its interactions with the densely hydrophilic lipopolysaccharide (LPS), a large glycolipid complex, decorating the surface of gram-negative bacteria such as *E. coli*. The teichoic acids and thick peptidoglycan component

of gram-positive bacteria such as the case with *S. aureus* are also hydrophilic, decreasing interactions with [¹⁸F]Sulfo-DBCO. As of now, it is not entirely evident nor can be conclusively determined why [¹⁸F]Sulfo-DBCO offers good percent ligation and little nonspecific binding.

C. Bacteria Concentration

Arguably one of the most important variables of the high-throughput assay, the concentration of bacteria must be highly monitored and regulated from a successful experimental execution standpoint.

Initial experiments utilized a 2:9 dilution of overnight bacterial cultures in LB, which may have quickly exhausted cellular nutrients. Because logarithmic-phase and stationary-phase bacteria express different proteins induced by gene expression patterns ultimately triggered by nutrient availability, metabolite labeling may have consequentially suffered from initial azide incubation in exhausted cell medium.

Despite an increased concentration of bacteria to media in later experiments (2:9 to 1:9 overnight culture to fresh LB), the lack of reconstituted medium may have placed bacteria in stationary or death phase upon subsequent metabolite incubation. This may explain our results in several ways:

If the bacteria were incubated with a metabolite in stationary-phase, the bacterial growth is slowed and cell wall synthesis is slowed, decreasing the demand for incorporating excess metabolite in the cell medium. This inherently decreases the amount of available azide for an alkyne click partner to ligate to in the latter half of the high-

throughput assay. Therefore, a large number of bacteria is not necessarily optimal to incorporate a greater amount of azide for SPAAC reaction.

In early instances, the OD_{600s} were observed to decrease at the end of metabolite incubation. Because D-alanine is an essential component in peptidoglycan synthesis and maintaining the cell wall structure, we wondered if high concentrations of altered D-alanine disrupted this conserved pathway or if the cell wall machinery could distinguish D-alanine modifications at high molar concentrations, triggering cell death. However, concentrations of up to 25 mM of D-azido-alanine had been reported to successfully incorporate in bacteria.²² This suggested that the cellular machinery for peptidoglycan synthesis was rather promiscuous and should have incorporated azide metabolite.

The drop-off in bacterial density suggests that cells lost the structural integrity of their cell walls as they began to enter the death phase. Cell death is often triggered by a loss of turgidity, resulting in cellular lysing where inner cytosolic components burst or seep out into the cell medium. It is possible that cellular fragments were pelleted and indiscriminately bound to incubated alkyne, resulting in observed nonspecific binding.

In the optimized high-throughput assay (**Figure 6**), a 1:100 overnight bacterial culture was required to see high, specific SPAAC reaction in *S. aureus*. Also of important note is the necessary bacterial reconstitution in fresh media with metabolite incubation. The fresh media contributed to rapid mid-log cell growth at the 1-hour mark, indicating bacteria were in a metabolically active state when incubated with metabolite. Moreover, *S. aureus* has been shown to grow more robustly in LB than F-12 due to a greater abundance of diverse nutrients, inducing different patterns of gene expression and cell growth patterns.²³ This matches our observed differences in greater alkyne ligation percentage in *S. aureus*

grown in LB compared to F-12. We can thereby extrapolate that the metabolic state of the bacteria is important to prime bacteria for modified metabolite uptake in important cellular pathways which is ultimately controlled by the concentration of bacteria in each incubation step of our optimized high-throughput assay.

However, despite an N=3 for the PET and optical arms, this experiment needs to be repeated and reevaluated for differences between *S. aureus* and *E. coli* as the cell wall makeup vastly differs in gram-positive and gram-negative bacteria.

D. PET vs. Optical Cyclooctyne Addition

The differential uptake between the optical experiments and the direct PET experiments are curious in that, we anticipate having different metabolic demand for D-amino acids by virtue of the different peptidoglycan content found in gram-positive and gram-negative pathogens. However, the direct PET experiments are gross in that it just informs on the uptake and not localization of the labeled D-amino acids. In contrast, the optical click experiments only identify what is on the cell surface when there may be a cytosolic component of azide accumulation that is unobservable. Moreover, it is important to note that by virtue of PET, the amount of alkyne is added in trace quantities, much less than what is added in optical experiments, which overwhelm the available azide sites. These observations underscore the need to look deeper at where the azido-D-amino acids reside as highlighted in Aim 2.

However, we would like to prioritize the use of positron emission as our observable signal, rather than optical. The positron emission is more amenable to our high throughput

assay and greater sensitivity can potentially be achieved. It also poses for greater potential for future clinical translation as opposed to optical probes.

Conclusion

The new PET tracer, [^{18}F]Sulfo-DBCO, readily labels bacteria when it undergoes SPAAC ligation on bacteria bearing its click partner, D-azido-alanine. This new [^{18}F] labeling technique to tag D-amino acids offers great versatility and general application in labeling gram-positive and gram-negative bacteria. This was done using a developed high-throughput *in vitro* assay which can be applied to canvas the chemical space in designing the next generation of [^{18}F] PET tracers. Though Aim 3 was not completed, versions of chemically modified D-alanine at the C-terminus are currently being synthesized and intermediates' identities have been confirmed by NMR. Much remains unknown, including the biochemical pathway of DAla in determining its metabolic fate (Aim 2). However, with an established protocol for a high-throughput assay with promising initial data, these aims can be accomplished relatively quickly.

References

1. Polvoy, I., Flavell, R. R., Rosenberg, O. S., Ohliger, M. A. & Wilson, D. M. Nuclear Imaging of Bacterial Infection: The State of the Art and Future Directions. *Journal of Nuclear Medicine* **61**, 1708–1716 (2020).
2. Parker, M. F. L. *et al.* Small molecule sensors targeting the bacterial cell wall. *ACS Infect Dis* **6**, 1587–1598 (2020).
3. Prescher, J. A. & Bertozzi, C. R. Chemistry in living systems. *Nat Chem Biol* **1**, 13–21 (2005).
4. Shieh, P. & Bertozzi, C. R. Design Strategies for Bioorthogonal Smart Probes. *Org Biomol Chem* **12**, 9307–9320 (2014).
5. Ordonez, A. A. *et al.* Molecular imaging of bacterial infections: Overcoming the barriers to clinical translation. *Science Translational Medicine* **11**, (2019).
6. Eggleston, H. & Panizzi, P. Molecular Imaging of Bacterial Infections in vivo: The Discrimination between Infection and Inflammation. *Informatics* **1**, 72–99 (2014).
7. Parker, M. F. L. *et al.* Sensing Living Bacteria in Vivo Using d-Alanine-Derived ¹¹C Radiotracers. *ACS Cent. Sci.* **6**, 155–165 (2020).
8. Stewart, M. N. *et al.* High Enantiomeric Excess In-Loop Synthesis of d-[methyl-¹¹C]Methionine for Use as a Diagnostic Positron Emission Tomography Radiotracer in Bacterial Infection. *ACS Infect. Dis.* **6**, 43–49 (2020).
9. Mutch, C. A. *et al.* [¹¹C]Para-Aminobenzoic Acid: A Positron Emission Tomography Tracer Targeting Bacteria-Specific Metabolism. *ACS Infect. Dis.* **4**, 1067–1072 (2018).

10. Weinstein, E. A. *et al.* Imaging Enterobacteriaceae infection in vivo with 18F-fluorodeoxysorbitol positron emission tomography. *Sci Transl Med* **6**, 259ra146 (2014).
11. Egan, A. J. F., Errington, J. & Vollmer, W. Regulation of peptidoglycan synthesis and remodelling. *Nat Rev Microbiol* **18**, 446–460 (2020).
12. Rivera, S. L. *et al.* Chemically Induced Cell Wall Stapling in Bacteria. *Cell Chemical Biology* **28**, 213-220.e4 (2021).
13. Automated Synthesis and Uptake Analysis of D-[Methyl-11C]-Methionine | Protocol. <https://www.jove.com/v/61705/automated-synthesis-and-uptake-analysis-of-d-methyl-11c-methionine>.
14. Neumann, K. D. *et al.* Imaging Active Infection in vivo Using D-Amino Acid Derived PET Radiotracers. *Sci Rep* **7**, 7903 (2017).
15. Vaidyanathan, G. & Zalutsky, M. R. Synthesis of N-succinimidyl 4-[18F]fluorobenzoate, an agent for labeling proteins and peptides with 18F. *Nat Protoc* **1**, 1655–1661 (2006).
16. Bouvet, V., Wuest, M. & Wuest, F. Copper-free click chemistry with the short-lived positron emitter fluorine-18. *Org. Biomol. Chem.* **9**, 7393–7399 (2011).
17. Shalizi, A., Wieggers, T. N. & Maamar, H. Click-to-Capture: A method for enriching viable *Staphylococcus aureus* using bio-orthogonal labeling of surface proteins. *PLOS ONE* **15**, e0234542 (2020).
18. Liechti, G. *et al.* A new metabolic cell wall labeling method reveals peptidoglycan in *Chlamydia trachomatis*. *Nature* **506**, 507–510 (2014).

19. Li, W. *et al.* Fluorodibenzocyclooctynes: A Trackable Click Reagent with Enhanced Reactivity. *Chemistry – A European Journal* **25**, 10328–10332 (2019).
20. Spangler, B. *et al.* Molecular Probes for the Determination of Subcellular Compound Exposure Profiles in Gram-Negative Bacteria. *ACS Infect. Dis.* **4**, 1355–1367 (2018).
21. Gershoni, J. M. & Palade, G. E. Electrophoretic transfer of proteins from sodium dodecyl sulfate-polyacrylamide gels to a positively charged membrane filter. *Analytical Biochemistry* **124**, 396–405 (1982).
22. Fugier, E. *et al.* Rapid and Specific Enrichment of Culturable Gram Negative Bacteria Using Non-Lethal Copper-Free Click Chemistry Coupled with Magnetic Beads Separation. *PLOS ONE* **10**, e0127700 (2015).
23. Missiakas, D. M. & Schneewind, O. Growth and Laboratory Maintenance of *Staphylococcus aureus*. *Curr Protoc Microbiol* **CHAPTER 9**, Unit-9C.1 (2013).

Publishing Agreement

It is the policy of the University to encourage open access and broad distribution of all theses, dissertations, and manuscripts. The Graduate Division will facilitate the distribution of UCSF theses, dissertations, and manuscripts to the UCSF Library for open access and distribution. UCSF will make such theses, dissertations, and manuscripts accessible to the public and will take reasonable steps to preserve these works in perpetuity.

I hereby grant the non-exclusive, perpetual right to The Regents of the University of California to reproduce, publicly display, distribute, preserve, and publish copies of my thesis, dissertation, or manuscript in any form or media, now existing or later derived, including access online for teaching, research, and public service purposes.

DocuSigned by:

Arya Mani

1B6E5B7D5B12421...

Author Signature

8/30/2021

Date